Research Journal of Biological Sciences 4 (9): 1056-1060, 2009
ISSN: 1815-8846

Antibacterial Effect of Synthesized Silver/Montmorillonite Nanocomposites by UV-Irradiation Method

[1]Mansor Bin Ahmad, [2]Majid Darroudi, [1]Kamyar Shameli, [1]Abdul Halim Abdullah,
[1]Nor Azowa Ibrahim, [3]Azizah Abdul Hamid and [3]Mohsen Zargar
[1]Department of Chemistry, Faculty of Science,
Putra Malaysia University, 43400 Serdang, Selangor, Malaysia
[2]Laboratory of Advanced Materials and Nanotechnology, Institute of Advanced Technology (ITMA),
Putra Malaysia University, 43400 Serdang, Selangor, Malaysia
[3]Department of Food Science, Faculty of Food Science and Biotechnology,
Putra Malaysia University, 43400 Serdang, Selangor, Malaysia

Abstract: Silver nanoparticles (Ag-NPs) were successfully synthesized into the interlayer space of Montmorillonite (MMT) by UV-irradiation method. $AgNO_3$ and Montmorillonite (MMT) were used as a silver precursor and solid support, respectively. The properties of Ag/MMT nanocomposites were studied as a function of UV-irradiation time. UV-irradiation disintegrated the Ag NPs into smaller size until a relatively stable size and size distribution were achieved. The UV-vis spectra of synthesized Ag-NPs showed that the intensity of the maximum wavelength of the plasmon peaks increased with increasing UV-irradiation time. The synthesized Ag/MMT nanocomposites under longer UV irradiation time are very stable over a long time in aqueous solution without any sign of agglomeration or precipitants. The crystalline structure of the Ag-NPs and basal spacing of MMT and Ag/MMT were also studied by Powder X-Ray Diffraction (PXRD). The antibacterial activity of Ag-NPs was investigated against Gram-negative bacteria (*Escherichia coli* and *Klebsiella pneumoniae*) and Gram-positive bacteria (*Staphylococcus aureus* and Methicillin-Resistant *Staphylococcus aureus* (MRSA)) by disk diffusion method using Muller-Hinton Agar (MHA) at different sizes of Ag-NPs. All of synthesized Ag-NPs were found to have high antibacterial activity. These results showed that Ag-NPs can be useful in different biomedical research and applications such as diagnostic and surgical devices, contrast agents, drug delivery vehicles and physical therapy applications.

Key words: Silver nanoparticles, montmorillonite, nanocomposite, UV-irradiation, antibacterial activity, muller-hinton agar

INTRODUCTION

The importance and investigation on the antibacterial activity of silver nanoparticles (Ag-NPs) is because of the increase in resistant of bacteria against classic and most strong antibiotics (Lee *et al*., 2005; Panacek *et al*., 2006). The Ag-NPs interactions with bacteria are dependent on the size and shape of the nanoparticles but bactericide mechanism of Ag-NPs is not clear (Morones *et al*., 2005; Pal *et al*., 2007). The antibacterial activity of the Ag-NPs can be used in several biomedical applications, for example, to reduce infections in burn treatment (Ulkur *et al*., 2005), dental materials and human skin (Bosetti *et al*., 2002; Gauger *et al*., 2003). MMT as lamellar clay has intercalation, swelling and ion exchange properties. Its interlayer space has been used for the synthesis of nanoparticles materials and biomaterials, as support for anchoring transition-metal complex catalysts and as adsorbents for cationic ions (Kozak and Domka, 2004).

In this research, the size effect of Ag-NPs on antibacterial property is presented. Via this method, we are able to obtain Ag-NPs with different sizes and antibacterial activity by controlling the UV-irradiation time.

MATERIALS AND METHODS

All reagents were of analytical grades and were used as received without further purification. $AgNO_3$ (99.98%), used as silver precursor, was supplied from Merck, Germany. MMT used as a solid support for Ag-NPs, was purchased from Kunipa-F, Japan. All aqueous solutions were prepared with Double Distilled water (DD-water).

Corresponding Author: Mansor Bin Ahmad, Department of Chemistry, Faculty of Science, Putra Malaysia University, 43400 Serdang, Selangor, Malaysia

Synthesis of Ag/MMT nanocomposites: The Ag/MMT nanocomposites were synthesized according to the previous research (Darroudi *et al*., 2009). Briefly, for the synthesis of Ag Nps, 5.0 g of MMT was dispersed in 500 mL double distilled water and vigorously stirred for 1 h. Five hundred milliliter aqueous solution of $AgNO_3$ (0.02 M) was added into the MMT aqueous suspension and the mixture was further stirred for 1 h. The dispersion was irradiated using the UV reactor with UV lamp at λ = 365 nm, while it was stirred at speed of 195 rpm. The irradiation times of 1 h (S1), 3 h (S2), 18 h (S3), 48 h (S4) and 96 h (S5) were applied for different cuvettes, respectively. Then, the suspensions of Ag/MMT were separated by centrifugation at speed of 15000 rpm for 15 min, washed with DD-water twice and dried under vacuum overnight. All experiments were conducted at ambient temperature.

Evolution of antibacterial activity: *In vitro* antibacterial activity of the samples was evaluated by disc diffusion method using Mueller-Hinton Agar (MHA) with determination of inhibition zones in millimeter (mm), which conforms to the recommended standards of the National Committee for Clinical Laboratory Standards (NCCLS). *Escherichia coli* (ATCC 25922), *Staphylococcus aureus* (ATCC 25923), Methicillin-Resistant *Staphylococcus aureus* (MRSA) (ATCC 700689) and *Klebsiella pneumoniae* (ATCC 13883) were used for reference of antibacterial effect assay. Briefly, sterile paper discs (6 mm) impregnated with 20 μL of MMT/Ag nanocomposites (S2, S4 and S5) suspended in normal saline and were left to dry in 37°C for 24 h in sterile condition. Bacterial suspension prepared by making a saline suspension of isolated colonies selected from an 18-24 h tryptic soy agar plate. The suspension was adjusted to match the tube 0.5 McFarland turbidity standard using spectrophotometer in 600 nm, which equal to 1.5×10^8 Colony-Forming Units (CFU)/mL.

The surface of MHA was completely inoculated using sterile swab, which steeped in prepared suspension of bacterium. Finally, impregnated discs were placed on the inoculated agar and the petri dish was incubated at 37°C for 24 h. After incubation the diameter of growth inhibition zones were measured. Chloramphenicol (30 μg) and Cefotaxime (30 μg) were used as positive standards in order to control the sensitivity of the bacteria.

Characterization: The Ag/MMT nanocomposites were characterized by Ultraviolet-Visible (UV-vis) spectroscopy, Transmission Electron Microscopy (TEM) and Powder X-Ray Diffraction (PXRD). The UV-vis spectra were recorded over the range of 300-700 nm by a Lambda 25-Perkin Elmer UV-vis spectrophotometer. TEM observations were carried out on a Hitachi H-7100 electron microscopy and the particle size distributions were determined using the UTHSCSA Image Tool software, Version 3.00 program. The structures of produced Ag/MMT nanocomposites were carried out on a Philips PXRD (X'pert, Cu K_α radiation). The change in interlamellar spacing of MMT and Ag/MMT nanocomposite were also studied by using PXRD in the small angle range of $2°<2\theta<12°$. The PXRD patterns were recorded at a scan speed of 2° min^{-1}.

RESULTS AND DISCUSSION

The colour of $AgNO_3$/MMT suspensions through reduction process by UV-irradiation changed from colourless to light brown, then to brown and finally to green, indicating the formation Ag-NPs in MMT suspension. The stability of synthesized MMT suspensions containing Ag-NPs was studied and indicated that S4 and S5 were very stable over a long time (>3 months) in aqueous solution without any sign of precipitants.

Figure 1 shows the TEM images and their corresponding size distributions of produced Ag-NPs under UV light for selected irradiation times. For S2, photo-reduced Ag-NPs are formed with a broad size distribution and mean particle size of about 30.53 nm (Fig. 1a and b). As it can be seen from Fig. 1c and d, for S4, the mean particles size of Ag-NPs were decreased considerably to 6.01 nm as compared to S2.

It can be seen that the larger Ag-NPs was obtained under shorter irradiation time and it was disintegrate under the further irradiation of UV light (Huang and Yang, 2008). As shown in Fig. 1e and f, in S5, no large decrease in the particle size and change in size distribution can be observed, when compared with S4. This indicates that the Ag-NPs obtained in this irradiation time are extremely stable.

The comparison between PXRD patterns of MMT and prepared Ag/MMT nanocomposite under chemical reduction route in the small angle range of 2θ ($2°<2\theta<12°$) indicates the formation of the intercalated structure (Fig. 2). The original d-spacing (d_L) of MMT, 1.24 nm is increased to 1.41 nm at smaller 2θ angles (2θ = 6.79° for S5) by silver intercalation. This d_L value is direct proof of the fact that, in the path of ion exchange, Ag^+ ions are bound not only on the external surfaces and edges of MMT but also in the interlamellar space. Metallic nanoparticles formed at the latter location are to cause of the increase in basal spacing. In these samples, the intensities of the reflections are significantly lower

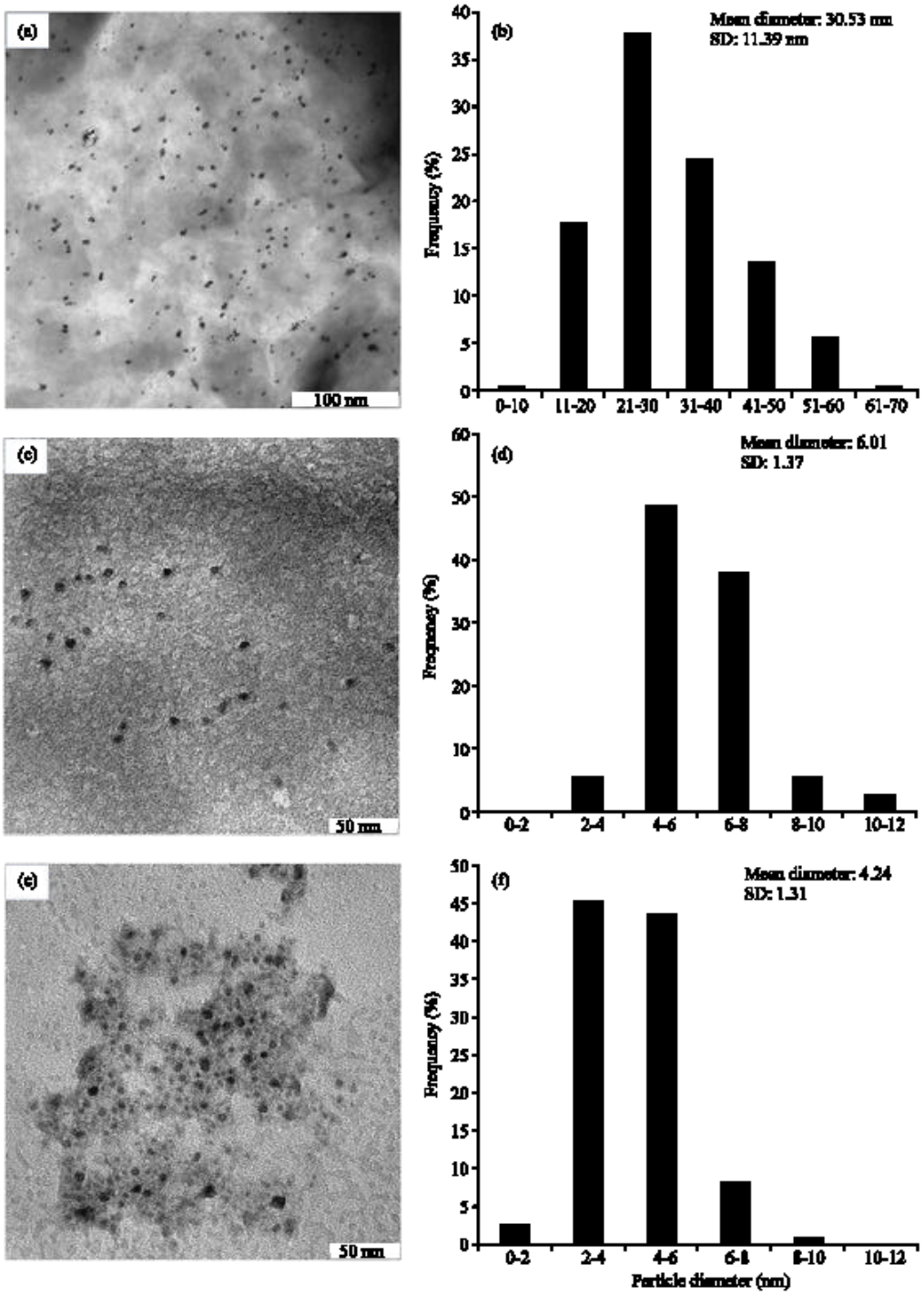

Fig. 1: TEM images and their corresponding particle size distributions of Ag-NPs at different UV-irradiation times; (a and b) S2, (c and d) S4 and (e and f) S5

whereas their half-widths are larger than those of undoped clay minerals: the highly ordered parallel lamellar structure of the mineral is disrupted by particle formation (Patakfalvi *et al*., 2003).

The PXRD patterns were also employed to determine the crystalline structures of the photo-reduced Ag NPs. As shown in Fig. 3, the PXRD peaks at 2θ of 38.2, 44.3 and 64.5° can be attributed to the (111), (200) and (220)

Table 1: Average of inhibition zones for synthesized Ag/MMT nanocomposites

	Inhibition zone (mm)			Control negative (mm)	Control positive (mm)	
Bacteria	S2	S4	S5	----------MMT----------	Cefotaxime	Chloramphenicol
E. coli	9.5	9	8.5	NA*	23	19
S. aureus	11.0	11	10.5	NA	28	20
MRSA	10.0	10	10.0	NA	30	21
K. pneumoniae	9.5	9	9.0	NA	31	25

*Not appear

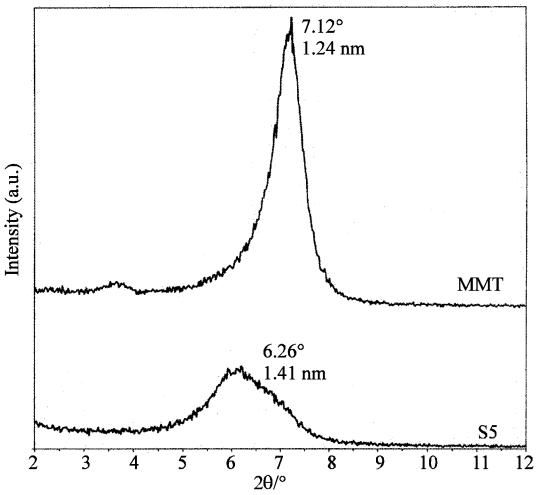

Fig. 2: PXRD patterns of MMT and Ag/MMT (S5) for determination of d-spacing (d_L)

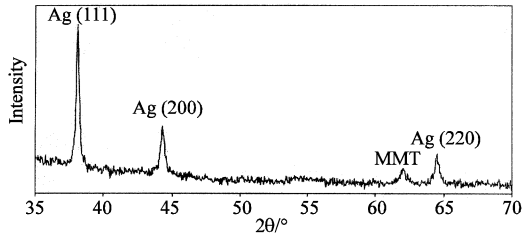

Fig. 3: PXRD pattern of Ag/MMT nanocomposite (S5)

crystallographic planes of face-centered cubic (fcc) silver crystals, respectively (Temgire and Joshi, 2004). The PXRD peak broadenings of Ag-NPs are mostly due to the presence of nano-sized particles in these nanocomposites (Prasad *et al*., 2006). In addition, there is a characteristic peak in about $2\theta = 62.1°$ that related to MMT clay (PXRD Ref. No. 00-003-0010) as a stable substrate.

The UV-vis absorption spectra of MMT-based Ag-NPs are shown in Fig. 4. The characteristic silver Surface Plasmon Resonance (SPR) band was detected around 360 nm, when the UV-irradiation time exceeded 3 h. In S3 and S4, the absorbance was increased and was slightly blue-shifted to 350 nm due to decrease particle size of Ag-NPs because absorption peak due to SPR of metal nanoparticles shows the blue-shift with

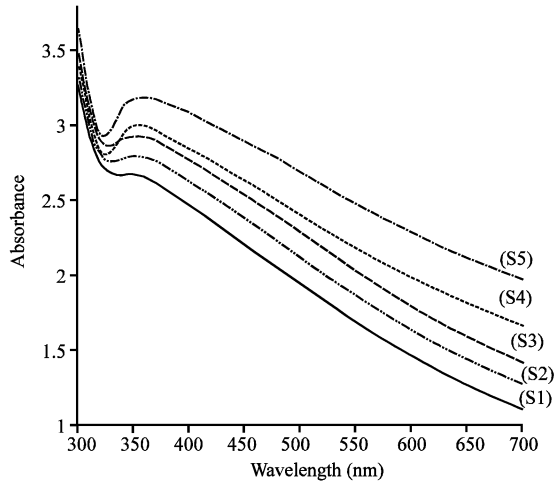

Fig. 4: UV-vis absorption spectra of Ag/MMT nanocomposites at different UV-irradiation times

decreasing in the particle size (Heath, 1989). In S5, the absorbance was considerably increased and was red-shifted to 360 nm. Higher concentration of metal nanoparticles may also lead to the red-shift of SPR band (Liu *et al*., 2007).

Inhibition zones values were obtained for the synthesized nanoparticles tested against *E. coli*, *S. aureus*, MRSA and *K. pneumoniae*. The results are presented as average values in Table 1.

Table 1 show that the Ag-NPs give high and similar antibacterial activity against Gram-positive and Gram-negative bacteria. Because of their size, Ag-NPs can easily reach the nuclear content of bacteria and they present the greatest surface area; therefore the contact with bacteria is the greatest (Lok *et al*., 2006). The Ag/MMT sols were used in the form in which they had been prepared. Therefore, antibacterial tests of solutions containing the reaction components were performed.

CONCLUSION

Ag-NPs with different sizes were synthesized in interlayer of MMT in an aqueous solution by UV-irradiation method and characterized using TEM, PXRD

and UV-vis absorption spectroscopy. The antibacterial properties of these nanoparticles to several Gram-positive and Gram-negative bacteria including multiresistant strains were successfully demonstrated.

REFERENCES

Bosetti, M., A. Masse`, E. Tobin and M. Cannas, 2002. Silver coated materials for external fixation devices: *In vitro* biocompatibility and genotoxicity. Biomaterials, 23: 887-892. DOI: 10.1016/S0142-9612(01) 00198-3. PMID: 11771707.

Darroudi, M., M.B. Ahmad, K. Shameli, A.H. Abdullah and N.A. Ibrahim, 2009. Synthesis and characterization of UV-irradiated silver/montmorillonite nanocomposites. Solid State Sci., 11: 1621-1624. DOI: 10.1016/j.solidstatesciences.2009.06.016.

Gauger, A., M. Mempel, A. Schekatz, T. Schafer, J. Ring and D. Abeck, 2003. Silver-coated textiles reduce *Staphylococcus aureus* colonization in patients with atopic eczema. Dermatology, 207: 15-21. DOI: 10.1159/ 000070935. PMID: 12835542.

Heath, J.R., 1989. Size-dependentsurface-plasmon resonances of bare silver particles. Phys. Rev. B., 40: 9982-9985. DOI: 10.1103/PhysRevB.40.9982.

Huang, H. and Y. Yang, 2008. Preparation of silver nanoparticles in inorganic clay suspensions. Compos. Sci. Technol., 68: 2948-2953. DOI: 10.1016/j. compsci-tech.2007.10.003.

Kozak, M. and L.J. Domka, 2004. Adsorption of the quaternary ammonium salts on montmorillonite. J. Phys. Chem. Solids, 65: 441-445. DOI: 10.1016/j.jpcs. 2003.09.015.

Lee, D., R.E. Cohen and M.F. Rubner, 2005. Antibacterial properties of Ag nanoparticle loaded multilayers and formation of magnetically directed antibacterial microparticles. Langmuir, 21: 9651-9659. DOI: 10.1021/ la0513306. PMID: 16207049.

Liu, F.K., Y.C. Hsu, M.H. Tsai and T.C. Chu, 2007. Using γ-irradiation to synthesize Ag nanoparticles: Mater. Lett., 61: 2402-2405. DOI: 10.1016/j.matlet.2006.07.193.

Lok, C.M., C.M. Ho, R. Chen, Q.Y. He, W.Y. Yu, H. Sun, P.K. Tam, J.F. Chiu and C.M. Che, 2006. Proteomic analysis of the mode of antibacterial action of silver nanoparticles. J. Proteome Res., 5: 916-924. DOI: 10. 1021/pr0504079. PMID: 16602699.

Morones, J.R., J.L. Elechiguerra, A. Camacho, K. Holt, J.B. Kouri, J.T. Rami'rez and M.J. Yacaman, 2005. The bactericidal effect of silver nanoparticles. Nanotechnology, 16: 2346-2353. DOI: 10.1088/0957-4484/16/10/ 059.

Pal, S., Y.K. Tak and J.M. Song, 2007. Does the antibacterial activity of silver nanoparticles depend on the shape of the nanoparticle? A study of the Gram-negative bacterium *Escherichia coli*. Appl. Environ. Microbiol., 73: 1712-1720. DOI: 10.1128/ AEM.02218-06. PMID: 17261510. PMCID: 1828795.

Panacek, A., L. Kvitek, R. Prucek, M. Kolar, R. Vecerova, N. Pizurova, V.K. Sharma, N. Tatjana and Z. Zboril, 2006. Silver colloid nanoparticles: Synthesis, characterization and their antibacterial activity. J. Phys. Chem. B., 110: 16248-16243. DOI: 10.1021/jp 063826h. PMID: 16913750.

Patakfalvi, R., A. Oszko and I. Dekany, 2003. Synthesis and characterization of silver nanoparticle/kaolinite composites. Colloids Surf A., 220: 45-54. DOI: 10. 1016/S0927-7757(03)00056-6.

Prasad, V., C.D. Souza, D. Yadav, A.J. Shaikh and N. Vigneshwaran, 2006. Spectroscopic characterization of zinc oxide nanorods synthesized by solid-state reaction. Spect. Chim. Acta A., 65: 173-178.

Temgire, M.K. and S.S. Joshi, 2004. Optical and structural studies of silver nanoparticles. Radiat. Phys. Chem., 71: 1039-1044. DOI: 10.1016/j.radphyschem.2003.10. 016.

Ulkur, E., O. Oncul, H. Karagoz, E. Yeniz and B. Celikoz, 2005. Comparison of silver-coated dressing (Acticoat™), chlorhexidine acetate 0.5% (Bactigrass®) and fusidic acid 2% (Fucidin®) for topical antibacterial effect in methicillin-resistant Staphylococci-contaminated, full-skin thickness rat burn wounds. Burns, 31: 874-877. DOI: 10.1016/j. burns.2005.05.002. PMID: 16011879.